FACIES	36	173-188	Pl. 47-51	2 Figs.	--	ERLANGEN 1997

Bacterial Origin of the Red Pigmentation in the Devonian Slivenec Limestone, Czech Republic

Bernard **Mamet**, Montréal, Alain **Préat** and Chantal **De Ridder**, Brussels

KEYWORDS: GEOBIOCHEMISTRY – RED PIGMENT – IRON-OXIDIZING BACTERIA – ENDOLITHIC PERFORATIONS – BARRANDIAN BASIN (CZECH REPUBLIC) – LOWER DEVONIAN (PRAGIAN)

SUMMARY

The deep-red lenses of the Pragian Slivenec Limestone have been extensively quarried for ornamental purposes since the XIIth century. Petrographic microscope observations indicate that the hematite stainings of the limestone follow ten different patterns.They range from massive non-directional filling of cavities to mineralized films and microstromatolites. Numerous iron-rich endolithes are observed. Some could be derived from bacterial or lichen perforations and some related to ferric bacteria. Infiltration along welded calcite crystals, regular mineralized films and microstromatolites suggest a ferric bacterial origin for the pigment. This is confirmed by scanning microscope examinations of polished sections, that show hematite concentrations along micrometric filamentous sheaths.

1 INTRODUCTION

Paleozoic red limestones ('red marbles') have been extensively quarried for centuries and used in architecture all over Western Europe. As they are scarce in nature, they are often used for decorative purposes e.g. church altars, pavements in palaces, mantlepieces in castles, pillars in cloisters. Among these ornamental stones in usage since the Middle Ages, one can cite the Devonian-Carboniferous Griottes of the Spanish and French Pyrenees (MIROUSE, 1992), the Frasnian red marbles of the Belgian Ardenne (BOULVAIN, 1993) and the Devonian Slivenec Limestone of the Barrandian Area in the vicinity of Prague (CHLUPÁC, 1968a, 1968b).

The origin of the red pigment has been a question of debate for a hundred years. For the Frasnian marbles, a detrital origin of the hematite has been accepted for a long time (see BOULVAIN, 1993 for references), but a microbial origin was supported by MONTY et al., 1982, MAMET & BOULVAIN, 1988 and BOULVAIN, 1993). The same origin was proposed for the Spanish Visean Griottes (MAMET & BOULVAIN, 1991) and for the Late Devonian French Griottes of the Pyrenees (MAMET & PERRET, 1995).

Iron bacteria offer an explanation to the paradox that hematite stained limestones formed in an paleoenvironment poor in iron and oxygen. This type of microbial geochemistry is now widely accepted (BEVERIDGE & DOYLE 1989; BIERLEY, 1990; MANN, 1992; EMERSON & REVSBECK, 1994).

The purpose of this article is to show that the red pigment of the Slivenec Limestone is also of bacterial origin.

2 REGIONAL STRATIGRAPHY

CHLUPÁC (1968a) reports on the Slivenec Marbles in the following terms: '...it was used as a technical term without stratigraphical significance ... to designate a well-known decoration and building stone exploited from the Middle Ages in the quarries at Cikánka in the Radotin Valley, S.W. of Slivenec near Prague.'

The stratigraphically restricted Slivenec Limestone designates a Lower Pragian (Lower Devonian) lithostratigraphic unit that is the lateral equivalent of the Upper Konesprusy and Lodenice-Reporyje Limestones.

Two outcrops have been investigated, the original Na Cikánka quarry mentioned above and the classical Berounka Valley Srbsko outcrops (Fig. 1).

Detailed description of the Na Cikánka stratigraphy is to be found in SVOBODA & PRANTL (1950), CHLUPÁC (1957), CHLUPÁC et al., 1985; CHLUPÁC et al., 1986 and CHLUPÁC (1988). Fifteen random samples were collected in the red lenses of the lower two meters of the Slivenec Marbles (beds 12-15 of CHLUPÁC et al., 1986, fig. 5, p.10). Ten other random

Addresses: Prof. B. Mamet; Université de Montréal, Faculté des Sciences, Département de Géologie, C.P. 6128, Succ. Centre-Ville, Montréal, H3C 3J7, Canada. Fax: Canada 1-514-343-5782; Prof. A. Préat, Université Libre de Bruxelles, D.S.T.E.-Géologie, CP160/02, 50 av. F.D. Roosevelt, B-1050, Brussels, Belgium. Fax: -32-2-650.22.26, E-mail: apreat@resulb.ulb.ac.be. Dr. Ch. De Ridder, Université Libre de Bruxelles, Laboratoire de Biologie Marine, CP160/15, 50 av. F.D. Roosevelt, B-1050, Brussels, Belgium. Fax: -32-2-650.27.96, E-mail: cridder@ulb.ac.be

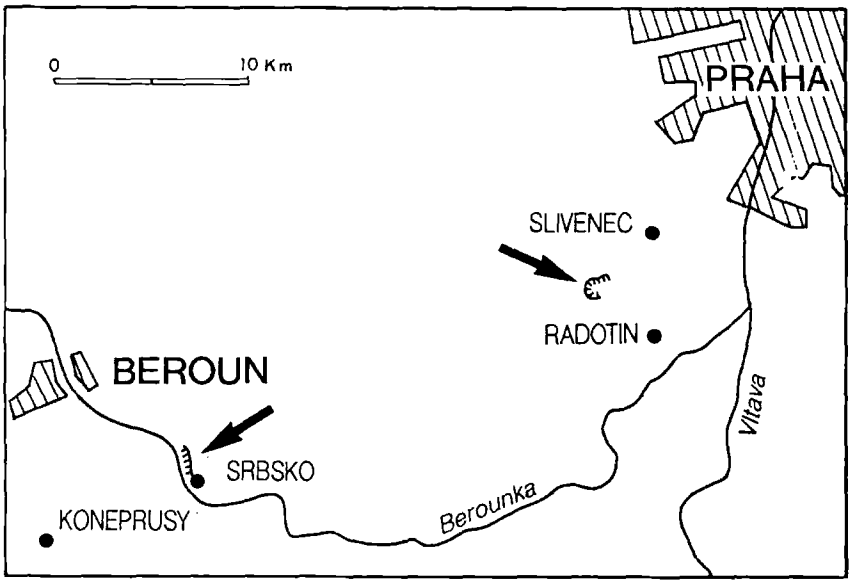

Fig. 1. Geographic location. Studied sections of Slivenec Limestone in cliffs northwest of Srbsko and in the Cikánka Quarry, northeast of Radotin.

samples come from the upper part of the exposure.

The lower samples are mostly pinkish-reddish, poorly sorted grainstones, with brachiopods, bryozoans and floated dacryoconarid 'tentaculites' (*Nowakia*). Trilobite fragments are extensively bored by sponges. The upper samples are reddish wackestones, with abundant sponge spicules and fewer 'tentaculites'.

These characters indicate marine conditions close to storm wave base. The red lenses are surrounded by green limestones of similar lithology, but where the iron matrix is reduced.

The classical Berounka Valley outcrops are described by SVOBODA & CHLUPÁC *in* SVOBODA et al., 1966. A photograph of the outcrop is to be found, plate XLIV, fig.2. Further details are in CHLUPÁC (1988). The Slivenec Limestone crops out under the Barrandova Cave, overlying the Koneprusy Limestone and underlying the Lodevice-Reporyje Limestones. Fifteen samples are derived from the red lenses in the lower 5 meters of the exposed section. Facies-wise they are very similar to the lower samples of the Na Cikánka Quarry.

In the two outcrops, the red lenses are embedded in grey-green limestones that, except for the colour, appear to have similar petrography. Thin-sections show fossils (brachiopod-bryozoan-'tentaculites') grainstones and spiculitic wackestones. They are hovewer a few differences. The grey-green facies is slightly more dolomitized, pyrite crystals are uniformly dispersed in the matrix, there is no trace of hematite and there is very little boring of the megafauna. Trilobite shells had abundant perforations filled by hematite in the red facies. Such borings are scarce in the grey-green facies and when present, are filled by recrystallized micrite.

In an attempt to explain the origin of the hematite pigment, we will first study its distribution with a petrographic microscope (order of magnification, 100x in three dimensions). We will then switch to the scanning microscope (order of magnification, 10000x in planar conditions) and conclude with one single hypothesis.

3 DISTRIBUTION OF THE HEMATITE

In thin sections and under microscopic observations, the hematite staining of the red Slivenec is not uniform, but follows nine sedimentary patterns. A tenth mode, diagenetic, will only be briefly mentioned.

1° Non-directional, random filling of pre-existing open cavities,

2° Replacement of pitted, syntaxial calcite in echinoderm plates and crinoid ossicles,

3° Infiltration following pre-existing calcite structures,

4° Filling of sponge borings,

5° Infiltration in endolithic filaments and original filaments,

6° Massive, irregular coatings,

7° Single mineralized films,

8° Multi-layered mineralized films and various microstromatolites,

9° Uniform dispersion in the spiculitic matrix,

10° Concentration along stylolites. This is clearly a diagenetic, post-sedimentation process and it will not be discussed any further.

1° Non-directional, random filling of pre-existing open cavities

The hematite is concentrated in former natural voids. Examples are bryozoan zooecia (scarce, Fig. 2/1, Pl. 47/11), whole ostracods with connected valves (very scarce, Fig. 2/2, Pl. 47/2), dacryoconarid 'tentaculites' (scarce, Fig. 2/3, Pl. 47/1), gastropod shells (scarce, Fig. 2/4, Pl. 47/3), trilobite spines (common, Fig. 2/5, Pl. 47/5, 8), echinid spines (common, Fig. 2/7, Pl. 47/4), and punctate brachiopods (common, filling of the punctae, Fig. 2/6, Pl. 47/7).

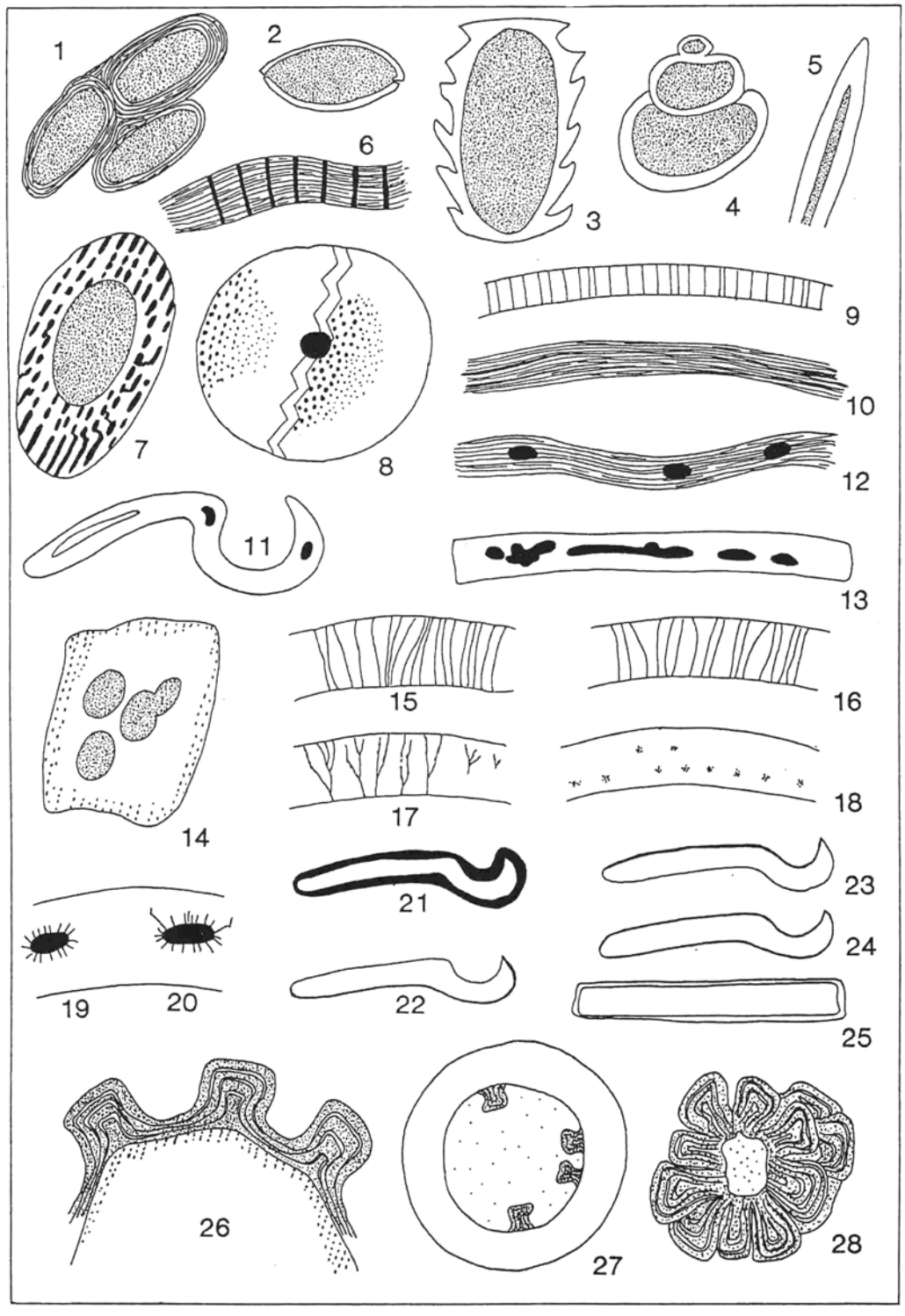

Fig. 2. Schematic representation of the distribution of the hematite. Refer to the text for explanation of the twenty-eight figures.

2° Replacement of pitted, syntaxial calcite in echinoderm plates and crinoid ossicles

During transportation and/or weathering, the syntaxial calcite filling of the echinoderm skeleton is replaced by micrite. In the Slivenec Limestone, the micritization is accompagnied by progressive hematitization. The process is centrifugal, uniform or centripetal (very common, Fig. 2/8, Pl. 47/6, 9, Pl. 50/6, 7).

3° Infiltration following pre-existing calcite structures

- Hematite infiltrations following the welded calcite prisms of trilobites. The infiltrations follow and enlarge the contact of the calcite crystals (common, Fig. 2/9, Pl. 49/6, 9). The same infiltrations are observed along the normal prismatic structures of mollusks (common, Pl. 48/2, Pl. 49/1);

- Hematite infiltrations following the foliated structure of brachiopod shells (scarce, Fig. 2/10, Pl. 49/5).

4° Filling of sponge borings (bioerosion)

- 'Dark', tubular cavities in trilobites (very common, Fig. 2/11, Pl. 47/10, Pl. 49/7, 8, 11, 14);
- 'Dark', tubular cavities in unpunctate, pseudopunctate or punctate brachiopod valves (common, Fig. 2/12, Pl. 47/7, Pl. 49/13, Pl. 50/10);
- 'Dark', tubular cavities in mollusks (common, especially among bivalves, Fig. 2/13, Pl. 48/2);
- 'Dark', tubular cavities in echinoderms (very common, as big 'blisters' filled by iron-rich micrite, Fig. 2/14, Pl. 47/6, 9).

Such bioerosion is rare or absent among bryozoans, ostracods, tentaculites.

5° Infiltration in endolithic filaments (cyanobacteria or lichen-induced). Probable iron-bacterial filaments.

- Even, long, sometimes curved, unbranched, thin filaments cutting through the welded calcite prims of trilobites or ostracods (common, Fig. 2/15, Pl. 48/1);
- Even, long, unbranched, thin filaments cutting through mollusk shells (common, Fig. 2/16, Pl. 48/2);
- Dichotomous or radiating filaments, uneven, with swells and strangulations cutting the partially dissolved structure of mollusk or trilobite fragments (common, Fig. 2/17, Pl. 48/10);
- Small hematite macula formed by the coalescence of micrometric spheres. By analogy to the 'melanospheric' structure of the stromatoporoids, they are named here 'erythrospheres' in reference to their colour (common, Fig. 2/18, Pl. 48/6-8, Pl. 50/9);
- Radiating, short filaments tufts, surrounding a sponge perforation. They are named here 'hedgehogs' (common, Figs. 2/19 and 20, Pl. 47/12, Pl. 48/10, 13-16, Pl. 49/2, 7, 8, 11, Pl. 50/5).

6° Heavy, massive, irregular coatings

Thick, undifferenciated hematite layer covering a trilobite or mollusk fragment (common, Fig. 2/21, Pl. 47/8, Pl. 48/8 at top).

7° Single mineralized films

- Even-layered, micrometric thick, regular hematite coating underlying a fossil fragment (common, Fig. 2/22 on a trilobite, Pl. 49/11);
- Even-layered, micrometric thick, regular hematite coating overlying a fossil fragment (common, Fig. 2/23 on a trilobite, Pl. 49/8, 12);
- Even-layered, micrometric thick, regular hematite coating completely surrounding a fossil fragment (common, Fig. 2/24, Pl. 49/5, 12).

8° Multilayered mineralized coatings and various microstromatolites

- Double (triple, quadruple ...) micrometric, regular hematite coatings separated by calcite bands (common, Fig. 2/25, Pl. 49/13, 14, Pl. 50/9, 10);

Plate 47 All illustrated specimens from the red lenses of the Slivenec Limestone, Early Devonian, Barrandium.

Fig. 1. Dacryoconarid shell completely filled by massive hematite. U. of M. 889/12, Cikánka Quarry, CZH19D, x 98

Fig. 2. Ostracod completely filled by massive hematite. U. of M. 887/36, Srbsko CZH1D, x 121

Fig. 3. Gastropod filled by massive hematite. U. of M. 887/22, Srbsko, CZH1D, x 78.

Fig. 4. Echinid spine completely filled by massive hematite. U. of M. 887/14, Srbsko, CZH1A, x 121

Fig. 5. Trilobite spine filled by massive hematite. Thin (4-5 µm) continuous peripheral hematite coating. U. of M. 887/14, Srbsko, CZH1A, x 121

Fig. 6. 1° Ferruginous micrite underlies the pitting of an echinoderm plate. Alteration increases from the periphery towards the center. 2° Ferruginous micrite fills the sponge borings. U. de M. 887/33, Cikánka Quarry, CZH19B, x 51

Fig. 7. Valve of punctate and ribbed brachiopod: 1° Punctae are filled by ferruginous micrite, 2° Sponge borings are also filled by ferruginous micrite, 3° Asymmetrical thick coating of the costae while the base of the valve is devoid of hematite. U. de M. 889/2, Cikánka Quarry, CZH24D, x 51

Fig. 8. Trilobite with heavy hematite coating and infilling. Thin hematite infiltrations along the calcite prisms of the wall. U. de M. 886/6, Cikánka Quarry, CZH23A, x 78

Fig. 9. Ferruginous micrite underlining the uniform pitting of an echinoderm plate. Irregular sponge borings filled by ferruginous micrite and microspar. U. de M. 889/11, Cikánka Quarry, CZH19D, x 31

Fig. 10. Trilobite fragment coated by a thick, irregular, asymmetrical layer of ferruginous micrite. Sponge cavity (to the left) filled by a thin hematite layer with hair-like endolithic perforations. Their growth is independent of the original prismatic structure. Later filling by ferruginous micrite. U. de M. 888/7, Cikánka Quarry, CZH23C, x 78

Fig. 11. Continuous, regular, hematite coating on a bryozoan fragment. Zooecia filled by hematite and ferruginous microspar. U. de M. 888/27, Cikánka Quarry, CZH24, x 121

Fig. 12. Trilobite fragment. 1° Thin, uniform coating at top and base, 2° Infiltrations along the contact of the calcite prisms, 3° Hematite filled sponge borings, 4° Radiating, short, filaments ('hedgehog'). U. de M. 889/27, Cikánka Quarry, CZH19B, x 300


1


2


3

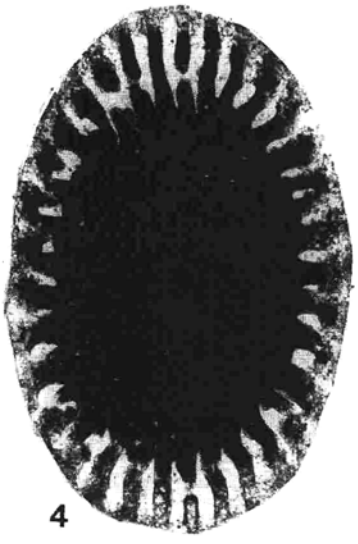
4


5


6


7


8


9


10


11

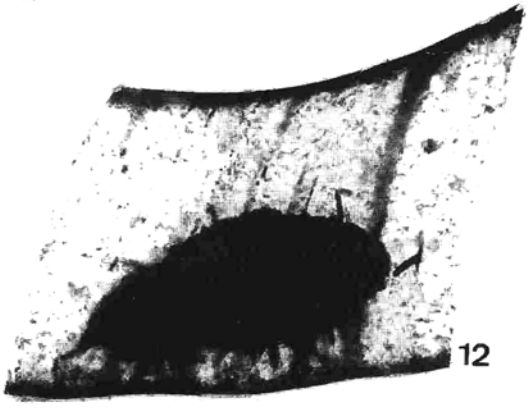
12

- Columnar microstromatolites surrounding a fossil fragment (growth symmetrical or asymmetrical, common, Fig. 2/26, Pl. 50/2, 3, 5, 6);
- Columnar microstromatolites growing inside a cavity (common, Fig. 2/27, Pl. 50/4);
- Crenulated oncoids (scarce, Fig. 2/28, Pl. 50/8).

9° Uniform dispersion in the spiculitic matrix

Observations from the SEM and Probe (see paragraph 6) show that the hematite is submicronic and at the limit of detection of the equipment. It is this extremely fine dispersion of the pigment in a much 'coarser' (micronic) micrite matrix, that produces the red colour.

4 FILAMENTS VS ENDOLITHES

As we have described in 5°, numerous types of micrometric filaments and spheres are encountered in trilobite and mollusk shells. This phenomenon is quite specific, as the same filaments are scarce among brachiopods and virtually absent in the rest of the macrofauna. Since they are coated by hematite, it would be tempting to infer that they are linked to iron bacteria. However other organisms such as the red algae (CAMPBELL et al., 1979), the cyanobacteria (AWRAMIK, 1982) and the lichens (FRIEDMAN, 1982, FRIEDMAN & WEED, 1987) also perforate carbonate substrates. These endolithic microcavities could be filled later on by iron oxides.

Red algae have filiform vegetative strands and irregular conchosporangial branches. This type of morphology is not observed in the Slivenec material and rhodophytes are to be discarded.

Endolithic cyanobacteria have long, constant filaments, usually unbranched. They could explain the 'hairy' filaments illustrated in Pl. 48/4. In addition, they have a slightly irregular outer contact which is common in cyanobacterial perforations.

Lichens hyphae have numerous dichotomies that could

Plate 48 All illustrated specimens from the red lenses of the Slivenec Limestone, Early Devonian, Barrandium.

Fig. 1. Trilobite fragment. Hair-like, hematite coated, upward growing, bacterial?, endolithic perforations. Filaments regular, continuous, non-dichotomous, about 2 µm thick.U. de M. 889/19, Cikánka Quarry, CZH19D, x 121

Fig.2. Mollusk fragment. Basal, regular hematite layer. Ferruginous coating between the calcite prisms. Irregular sponge borings. Straight and curved, 2 µm thick, bacterial endolithic filaments criss-cross the original structures. U. de M. 887/11, Srbsko, CZH1A, x 78

Fig. 3 is an enlargment of Fig. 1, x 300

Fig. 4. Mollusk fragment. Upward-growing, hairlike clusters of ferruginous coatings along the prismatic structures and straight, regular, 2-3 µm thick bacterial endolithic filaments. U. de M. 894/21, Srbsko, CZH1D, x 78

Fig. 5. Mollusk fragment. Central part with hematite filled sponge cavities. Lower end upper layer composed of small clusters of two- to six hematite spheres ('erythrosphere' layer).U. de M. 894/25, Cikánka Quarry, CZH19A, x 78

Fig. 6-7. Mollusk fragments with numerous 'erythrospheres'. U. de M. 888/13 and 13bis, Cikánka Quarry, CZH23D, x 121

Fig. 8. Mollusk fragment. Thick hematite coating at the top. Base irregular, gouged by an 'erythrosphere' layer. U. de M. 888/19, Cikánka Quarry, CZH19A, x 78

Fig.9. Trilobite fragment. Hematite filled sponge borings. Randomly distributed hair-like bacterial filaments. One oblique perforation (center right) is interrupted by the prismatic structure forming a 'T'. U. de M. 889/24, Cikánka Quarry, CZH19E, x 121

Fig. 10. Trilobite fragment. Continuous upper and lower thick hematite layer. Endolithic filaments generally grow upwards. They are irregular, dichotomous, and present swells and strangulations (diameter, 2-4 µm). U. de M. 889/13, Cikánka Quarry, CZH19D, x 121

Fig. 11. Trilobite fragment. Even basal hematite layer. Contacts of calcite prisms underlined by ferruginous infiltration. Sponge cavities surrounded by short endolithic perforations ('hedgehogs'). U. de M. 889/17, Cikánka Quarry, CZH19D, x 121

Fig. 12. Ostracod. Outside hematite coating poorly developed, while quite thick inside the valves. Original wall prismatic structure underlined by hematite. Some randomly-oriented perforations. U. de M. 889/6, Cikánka Quarry, CZH28, x 121

Fig. 13. Trilobite fragment. Detail of 'hedgehog' structure. Filamentous perforations straight. Diameter, 2 µm. U. de M. 889/26, Cikánka Quarry, CZH19B, x 300

Figs. 14-15. Trilobite fragments. Thin, discontinuous coating. Ferruginous micrite filled 'hedgehogs'. U. de M. 889/8 and 894/26, Cikánka Quarry, CZH19D, x 121

Fig. 16. Trilobite fragment. Thin, continuous, regular coating. Three coalescent 'hedgehogs' filled by ferruginous micrite. Some ferruginous infiltration underline the prismatic structure of the wall. U. de M. 888/1, Cikánka Quarry, CZH19B, x 121

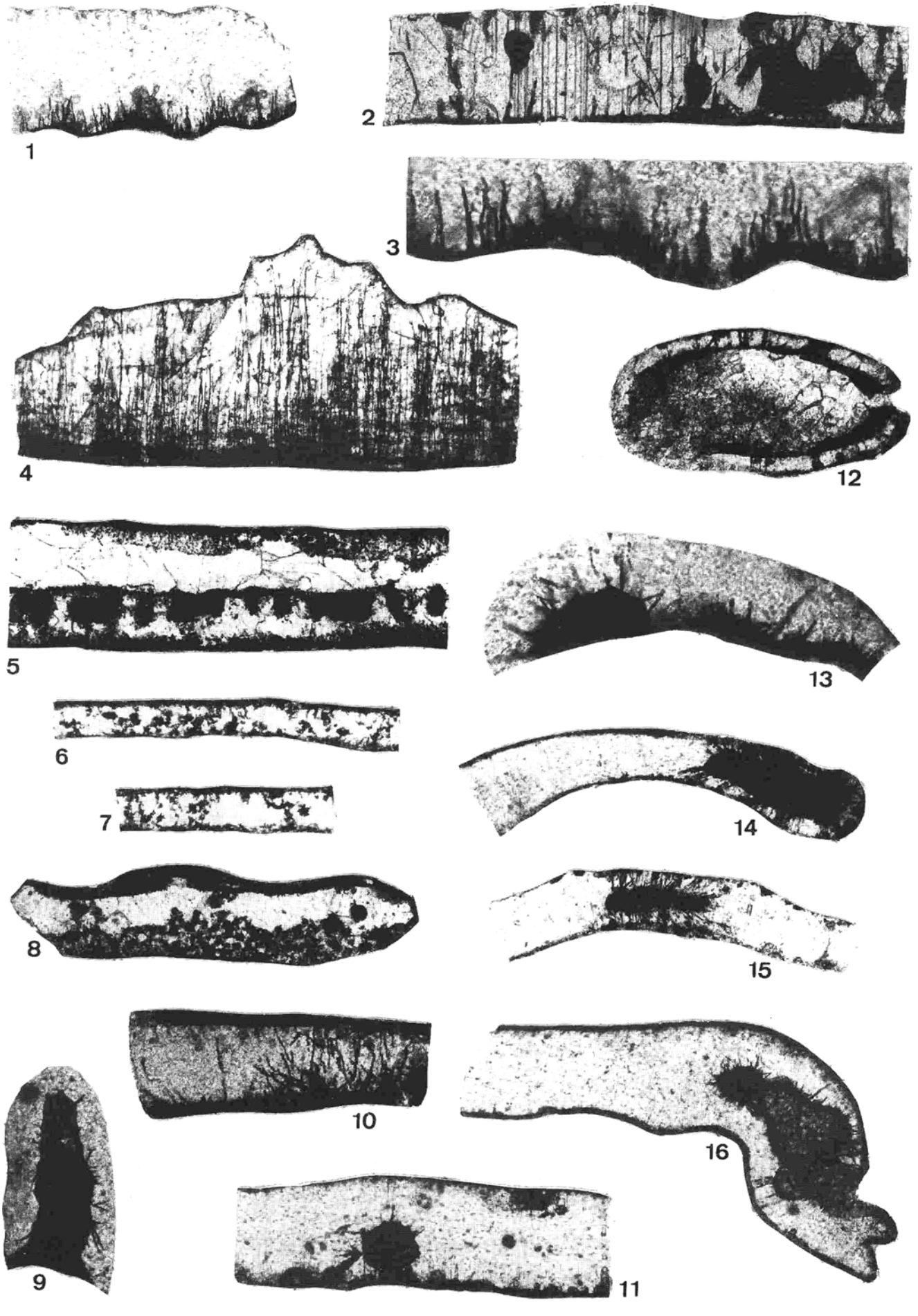
1
2
3
4
5
6
7
8
9
10
11
12
13
14
15
16

fit those observed in Pl. 48/1, and enlarged Pl. 48/3.

These structures are therefore not convincing proof of the existence of bacteria. On the other hand short, straight, simple radiating filaments surrounding the 'hedgehogs' could be ferric or iron-oxidizing strands (Pl. 48/13-16). Similarly, the hematite macula formed by the coalescence of microspheres have the same origin ('erythrospheres', Pl. 48/6, 7). Compare these Slivenec structures, with those illustrated by BOULVAIN, 1989, plate 1, figs. B, C and D from the Frasnian red marbles.

5 ORIGIN OF THE PIGMENTATION

As mentionned in the introduction, two hypotheses have been proposed to explain the red pigmentation. We have also described and illustrated nine types of original pigment distribution observed in thin sections.

A detrital origin is compatible with five of observed distributions, 1° filling of preexisting cavities, 2° replacement of syntaxial calcite, 4° filling of sponge borings, 6° formation of massive coatings, and 9° uniform dispersion.

The origin of filaments described in 5° is debatable. Part of them could be endolithic perforations, some of them are molds of iron bacteria.

A detrital origin is not compatible with the following points: 3° the micrometric infiltration along the contact of the calcite crystals (welded prismatic in the case of trilobites, mostly normal prismatic or cross-lamellar among mollusks). These infiltrations are highly specific and do not affect other representives of the macrofauna, 7° the formation of single-layered micrometric mineralized films. These films are not phototropic. They are observed as continuous layers as well as restricted to the upper or lower part of the fossil fragments. They also develop in 'dark' cavities, 8° the formation of multi-layered coatings and microstromatolites. Both are also non phototropic. Independent of light, they are formed in 'dark' cavities and are centripetal or centrifugal.

6 OBSERVATIONS FROM THE SCANNING MICROSCOPE

Polished thin sections were examined under the SEM (NORAN 1100/1110 RX Spectrometer and JEOL Superprobe

Plate 49 All illustrated specimens from the red lenses of the Slivenec Limestone, Early Devonian, Barrandium.

Fig. 1. Mollusk fragment with thin (1-2 µm) peripheric hematite coating. Infiltrations along the prism boundaries and hair-like endolithic perforations. U. de M. 894/17, Srbsko, CZH1C, x 121

Fig. 2. Trilobite fragment devoid of hematite coating. Bacterial filling reduced to a small 'hedgehog'. U. de M. 894/18, Srbsko, CZH1C, x78

Fig. 3. Regular, undifferentiated, thick hematite coating on a mollusk. U. de M. 887/29, Cikánka Quarry, CZH19, x 98

Fig. 4. Perforated trilobite spine. Regular, thin ferruginous micrite coating on outside and inside surfaces and in the perforations. Small 'hedgehog' at the top. U. de M. 888/2, Cikánka Quarry, CZH19C, x 78

Fig. 5. A rare example of hematite infiltration following the foliated layers of an unpunctate brachiopod. U. de M. 889/7, Cikánka Quarry, CZH28, x 78

Fig. 6. Normal prismatic calcite structure of a trilobite fragment underlined by hematite infiltration. U. de M. 888/12, Cikánka Quarry, CZH23D, x 121

Fig. 7. Very thin (2-3 µm) regular, continuous hematite coating surrounding a trilobite. Small 'hedgehog'. U. de M. 888/24, Cikánka Quarry, CZH24B, x 51

Fig. 8. Thin, regular hematite layer restricted to the top of a trilobite fragment. 'Hedgehogs' and irregular sponge perforations.'Erythrospheric' structures (upper left). Small 'hedgehog' at the top. U. de M. 889/1, Cikánka Quarry, CZH24D, x 38

Fig. 9. Heavy, irregular hematite layer surrounding a weathered trilobite fragment. Prismatic structures, perforations and 'hedgehogs' underlined by hematite. Small 'hedgehog' at the top. U. de M. 894/27, Cikánka Quarry, CZH19A, x 98

Fig. 10. Punctate brachiopod, heavily burrowed by sponges. Hematite and ferruginous microspar fill the punctae and the cavities. Simple microstromatolites cover the top of the valve. U. de M. 888/22, Cikánka Quarry, CZH24A, x 78

Fig. 11. Extensively perforated trilobite. Heavy hematite coating cover the top of the fragment. Prismatic structure unequally underlined. 'Hedgehogs' filled by ferruginous microspar. U. de M. 889/15, Cikánka Quarry, CZH19D, x 78

Fig. 12. Thin, uniform, single-layered hematite coating on a trilobite fragment. U. de M. 894/23, Srbsko, CZH1D, x 78

Fig. 13. Thin, uniform, two-layered hematite coating on a brachiopod valve. Sponge borings filled by ferruginous microspar. Some hematite infiltration between the foliated layers. U. de M. 898/18, Cikánka Quarry, CZH24A, x 51

Fig. 14. Thin, uniform, two-layered hematite coating on a trilobite fragment. Some sponge borings. U. de M. 889/4, Cikánka Quarry, CZH24D, x 78

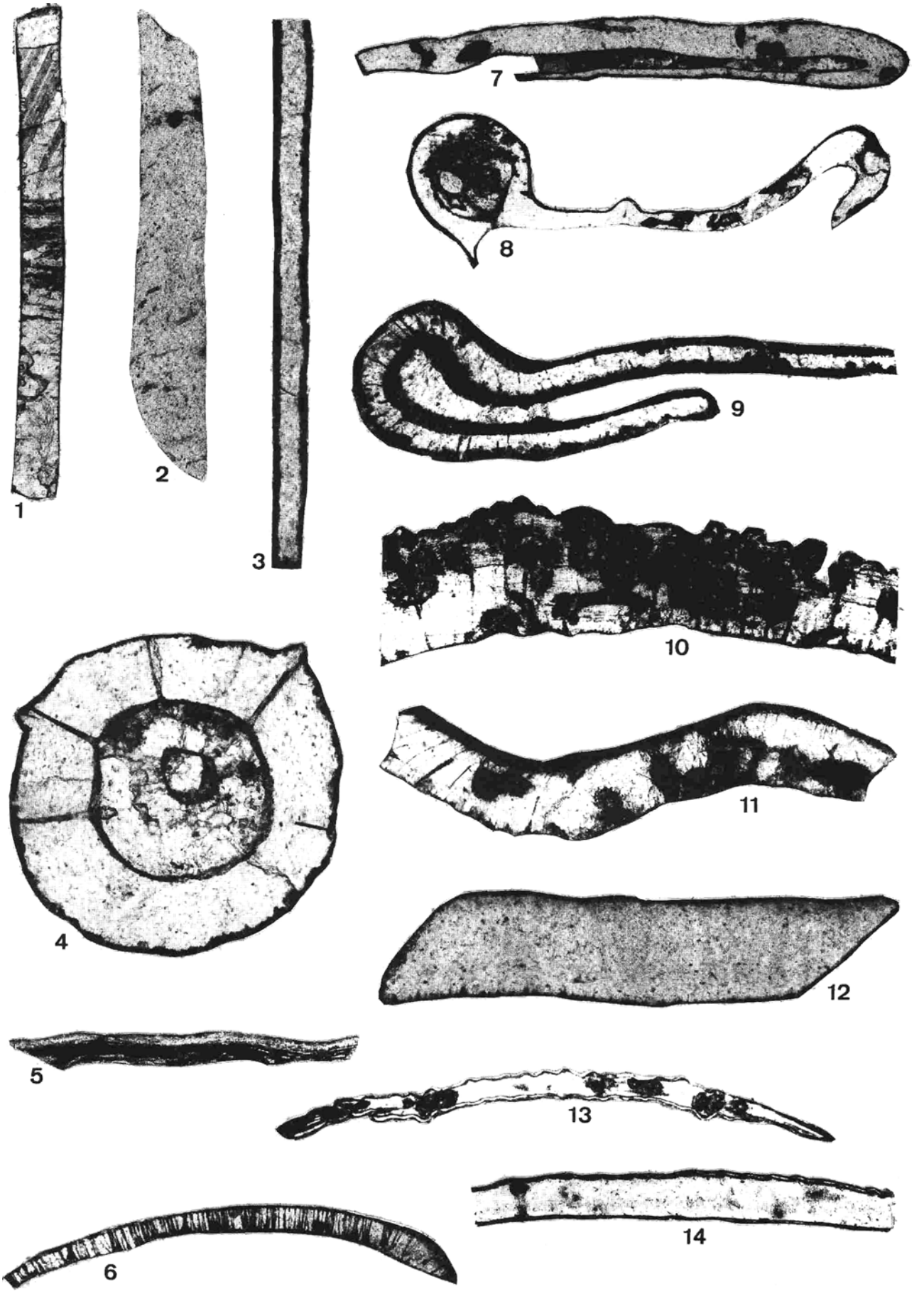
1
2
3
4
5
6
7
8
9
10
11
12
13
14

733) on preparations that were carbon coated by sputtering. The surface view of these preparations is significantly different from the views derived from classical optical microscopy. Due to the thickness of the thin sections (30 µm) all objects appearing by transparency seem well-formed and are visualized in 3-D. Under the SEM, only a small percentage (less than 3 %) of the whole objects is visible due to the high resolution of the device (i.e. 1 to 2 µm) restricted to the surface of the preparations. Since the majority of the objects are not planar at this scale they appear discontinuous and this complicates the geometrical reconstruction.

6.1 Observed morphologies

Two main types of bacteria-like material can be recognized: (1) filamentous bacteria in the form of straight or occasionally of spiral chains of bacilli and (2) coccoid bacteria in the form of small colonies or isolated cells.

6.1.1 The filamentous bacteria-like type (type 1)

This type is the most widespread form. It is represented by regular chains of cells enclosed in tubular brown to dark brown sheaths (Pl. 51/2-6). These sheaths are often attached to solid substrates (mainly mollusc and trilobite shells) or are developped inside inframillimetric bushes on a micritic matrix. The average sheath thickness is of about 0.2 to 0.5 µm, the cell diameter ranges from 2 to 3 µm and could have been smaller due to the weak degradation of the structure during diagenesis. The total width of the filament is a few microns (< 4 µm). All these thin sheaths are encrusted by iron (hematite) associated with very low concentrations of titanium and manganese. The chains are quite regular, reach over 100 µm, with occasional curved spiral forms. Some filaments have grown perpendicularly to other filament (Pl. 51/6).

6.1.2 The coccoid bacteria-like type (type 2)

Spherical to ovoid bodies that are partially or completely encrusted with iron oxides commonly occur (Pl. 51/1, 5). The average diameter of the bodies ranges between 1 and 2 µm. They occur as single body or short chains of a few elements. Thus they do not constitute long filamentous chains. They are commonly associated with the regular chain previously reported. A few of these bodies exhibit a ring-shaped habitus (< 0.5 µm in thickness) suggesting a capsule-like ring encrusted by iron oxide (Pl. 51/5). Larger bodies (7 µm in diameter) in the same figure could correspond to several cells surrounded by the same type of capsule. Under optical microscope, these bodies were coined 'erythrospheres'.

6.2 Interpretation and discussion

The microorganisms described in this work are filamentous or coccoid in shape and all of them are encrusted with ferric iron. Microorganisms coated with ferric iron precipitates are observed in several taxonomical groups, namely, Archaebacteria, Eubacteria, Fungi and Protozoans (Dahanayake & Krumbein 1986, Crichton,

Plate 50 All illustrated specimens from the red lenses of the Slivenec Limestone, Early Devonian, Barrandium.

Fig. 1. Trilobite spine. Outer periphery surrounded by a thin, continuous hematite layer that develops into simple microstromatolites. Inside cavity lined by thin, continuous hematite single layer with smaller build-ups. In the wall, prisms contacts underlined by centrifugal hematite infiltrations. Sponge borings filled by ferruginous microspar. U. de M. 889/3, Cikánka Quarry, CZH24D, x 78

Fig. 2. Trilobite fragment. Asymmetrical outer coating of 2-3 layers grading into incipient microstromatolites. U. de M. 888/25, Cikánka Quarry, CZH24B, x 121

Fig. 3. Perforated trilobite spine. Outer and inner surfaces covered by a thin hematite layer growing inward and outward into simple microstromatolites. U. de M. 888/26, Cikánka Quarry, CZH24B, x 121

Fig. 4. Partially dissolved dacryoconarid shell (*Nowakia*). Inside cavity coated by two hematite layers. Outside periphery coated by microstromatolites that develop on the ribs. Ferruginous micrite-filled sponge borings. U. de M. 888/28, Cikánka Quarry, CZH24B, x 98

Fig. 5. Four microstromatolites growing on a foliated brachiopod fragment. One small 'hedgehog' structure. U. de M. 888/14, Cikánka Quarry, CZH23D, x 121

Fig. 6. Asymmetrical growth of ferruginous microstromatolites on two sides of an altered echinoderm plate. The two other sides are devoid of coating. U. de M. 888/31, Cikánka Quarry, CZH24C, x 78

Fig. 7. Single row of uneven-shaped microstromatolites on an altered echinoderm plate. U. de M. 888/20, Cikánka Quarry, CZH24A, x 78

Fig. 8. Crenulated multi-layered oncolite. U. de M. 888/8, Cikánka Quarry, CZH23C, x 98

Fig. 9. Sponge-perforated trilobite fragment with 'erythrospheric' clusters. Two regular, thin hematite layers gradually passing into microstromatolites. U. de M. 888/21, Cikánka Quarry, CZH24A, x 78

Fig. 10. Sponge-perforated, foliated brachiopod valve. Two-three regular, thin hematite layers grade to microstromatolites at both ends. U. de M. 888/34, Cikánka Quarry, CZH24C, x 38

Fig. 11. Crenulated multi-layered microstromatolite. U. de M. 888/30, Cikánka Quarry, CZH24, x 98

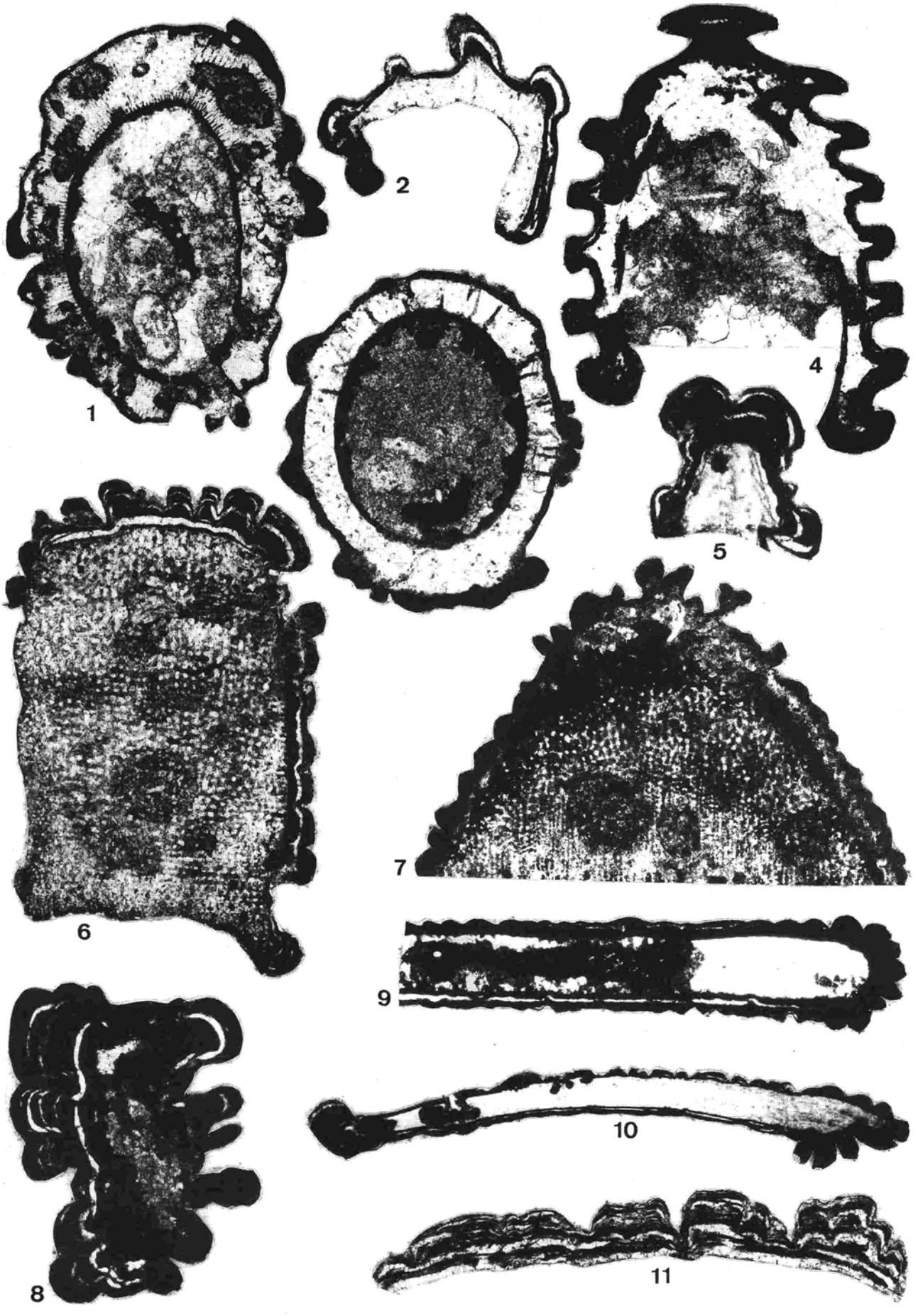
1
2
4
5
6
7
8
9
10
11

1991; BOULVAIN, 1993; BROCK et al.,1994). On the basis of their size and their morphology, the presently observed microorganisms resemble Eubacteria. Iron bacteria, i.e. bacteria traditionally considered as associated with ferric iron precipitates, occur in freshwater and marine environments. Remember that pH and oxygen are determinant factors in the form taken by iron in aqueous environments (CRICHTON, 1991). In the presence of oxygen, the soluble ferrous form of iron (Fe^{2+}) is stable at low pH (chemical oxidation is slow) while it is spontaneously oxidized to an insoluble ferric form (Fe^{3+}) at neutral pH. Therefore, solubility and thus availability of iron, is limited in oxic conditions. According to BROCK et al. (1994), few bacteria actively oxidize iron from the ferrous to the ferric state. Active iron-oxidation has been clearly demonstrated for acidophilic bacteria, i.e., for bacteria that are living at acid pH where ferrous iron is available in oxic environment. This is the case of *Thiobacillus ferroxidans* (Eubacteria) which lives in acid polluted environments as mineral or coal mining, and of *Sulfolobus* species (Archaebacteria) which lives in acid springs. These iron bacteria use the energy gained from the oxidation of ferrous to ferric iron for the reduction of carbon dioxide (chemolithoautotrophy) or facultatively of organic nutrients (mixotrophy). As the energy yielded by the reaction is low, large amount of iron must be oxidized and can lead to extensive deposits of ferric iron (RHEINHEIMER, 1980; BROCK et al., 1994). However, in addition to these bacteria, there are some other iron bacteria which grow at neutral pH. These bacteria are commonly living where ferrous iron is moving from anoxic to oxic conditions, namely at interfaces between anoxic and oxic environments (BROCK et al., 1994). The most commonly reported iron bacteria from neutral pH environments are the sheathed bacteria *Sphaerotilus natans* and *Leptothrix* species, and the stalked bacterium *Gallionella ferruginosa*. Among these, active iron oxidation coupled with chemoautotrophy has only been demonstrated for *G. ferruginosa*. For the others, the process involved in iron precipitation remains an open question.

Complexation of metal ions by the exopolymers produced by the bacteria has been suggested to play an important process in mineralization (SIMKISS & WILBUR, 1989; GEESEY & JANG, 1989). Indeed, many different types of bacteria (and of other microorganisms) produce extracellular polymeric substances (EPS) which form cellular coatings (glycocalyx) and presumably most of the slime matrix in biofims and bacterial mats. In bacteria, the glycocalyx may present various aspects of outer coverings as envelopes, capsules, sheaths (BROCK et al., 1994; NEU, 1994). The main components of these EPS are peptidoglycans, proteins and polysaccharides. It is the acidic groups (the more effective is the carboxyl residue) of the peptidoglycans and of the acidic polysaccharides that can bind metal ions such as iron ions (GEESEY & JANG, 1989; SIMKISS & WILBUR, 1989). EPS slow the diffusion of the metal ions and these react with the acidic residues of the EPS by direct binding or electrostatic interactions. Such a process of iron ion immobilization could be widespread among microorganisms producing EPS and could constitute a first step leading to further mineralization (GEESEY & JANG, 1989). According to the previous authors, ferrous and ferric ions can react with EPS and thus be trapped within microbial coatings. Ferrous ions can be subsequently oxidized by molecular oxygen (DECHO, 1994) or by oxidizing proteins as for *Leptothrix discophora* (CORSTJENS et al.,1992). Ferric ions mostly available to EPS are those from colloids (WELLS et al.,1995) or from organic complexes (EHRLICH, 1990). In addition, precipitation of ferric iron that has been initiated through complexation with EPS could go further through nucleation (DALAS, 1990).

Taking in account all these bibliographical data, one may suggest that ferric iron encrustment of microorganisms most presumably starts by a two steps process: (1) trapping by EPS , (2) oxidation of ions trapped in a reduced state. This oxidation can be spontaneous (in oxic environment) but it could also be biological (via chemoautotrophy or via oxidizing proteins). In this context, iron availability

Plate 51 All figures from the red lenses of the Slivenec Limestone, Cikánka Quarry, Early Devonian, Barrandium. SEM pictures on polished thin section, sample CZH19.

Fig. 1. Chain of spheroidal bodies (diameters 0.6 - 0.8 µm; see type-2 in text) with rod-shaped connections (diameters 0.3 µm). Bar is 4 µm.

Fig. 2. A partially decayed, deformed, iron-encrusted filament and a transverse cross section of an other. Original morphology observed on the top of the photograph. Bar is 20 µm.

Figs. 3-4 Bacterial filaments encrusted by hematite (white zones, width varying from 0.1 to 0.6 µm. The sheath? outlines the morphology of the barrel shaped bacteria cells (diameter 2 µm, length 2 - 3 µm). The cell separation is underlined by pseudo-septations. The dark background is formed by calcitic micrite. Hematite crystals are submicronic and not recognizable at the SEM magnification. Bar of 3 is 6 µm. Bar of 4 is 4 µm.

Fig. 5. V-shaped double filaments similar to figures 2 to 5 associated to spherical bodies (diameter 1.5 µm; see type-2 in text). Bar is 20 µm.

Fig. 6. Parallel-growing bacterial filaments perpendicular to a hematite substrate (also of bacterial origin?). The discontinuous aspect is due to the sinuous filaments. These are not in the plane of observed surface of the SEM. Cell morphology and pseudo-septations similar to figures 3 and 4. Bar is 20 µm.

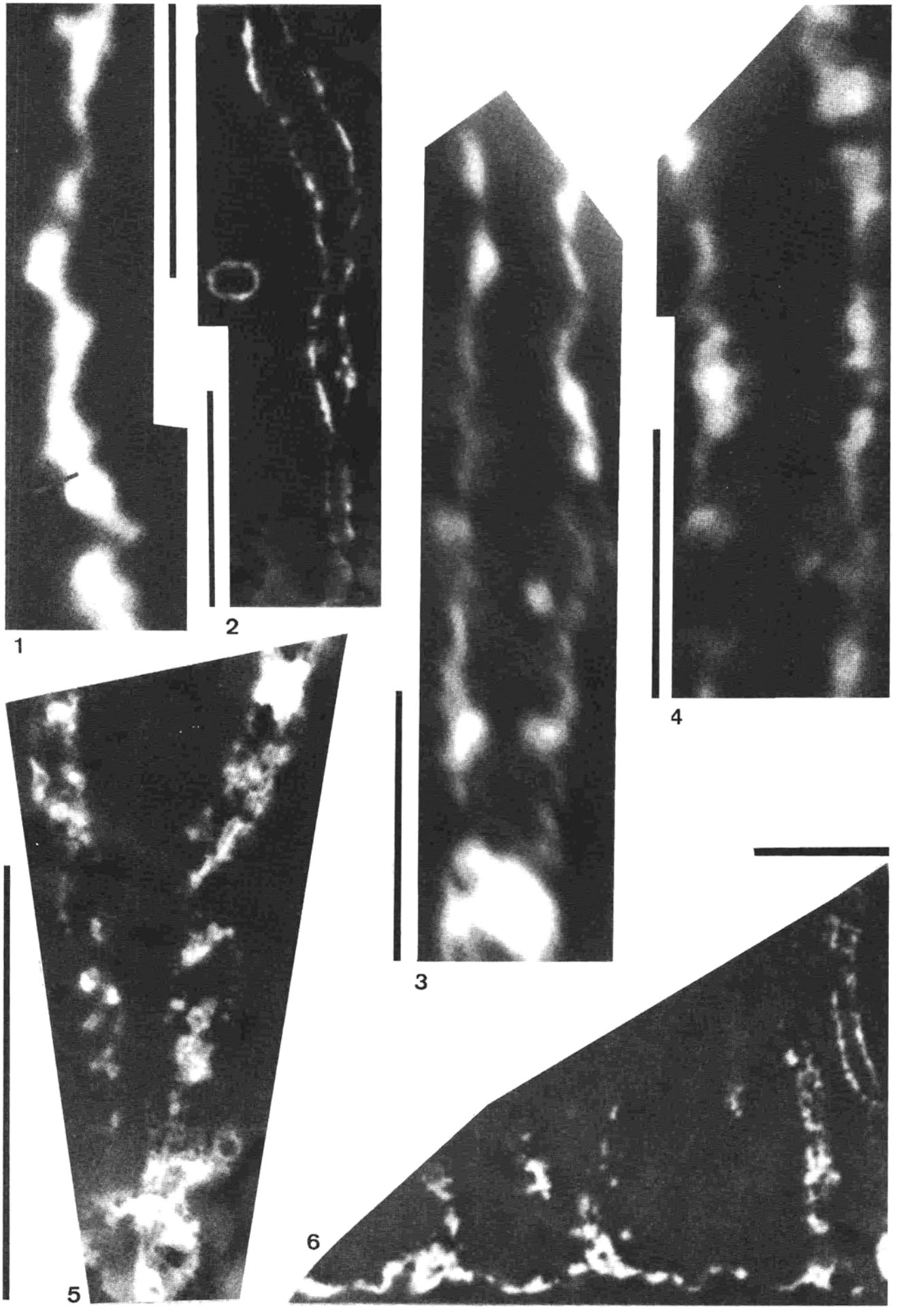
1
2
3
4
5
6

in the surrounding as well as the nature and abundance of the EPS produced must be two key factors at the basis of the development of ferric iron precipitates. In low pH environments, microbial chemoautotrophy (based on iron oxidation reaction as energy source) would be an additional factor.

In microbial mats from hydrothermal vents sites (JANNASCH & WIRSEN 1981; KARL et al., 1989; JUNNIPER et al., 1995) and in several types of other microbial mats and biofilms (see e.g., EMERSON & REVSBECH 1994 and BROWN et al., 1994; GILLAN & DE RIDDER 1995, respectively), ferric iron precipitates form in the glycocalyx that immediately surrounds the bacteria but also within the slime matrix between the bacterial cells. Such microbial communities can lead to local accumulation of ferric iron (GILLAN & DE RIDDER , 1995). In our samples filamentous and coccoid bacteria occur together and most probably have been members of a biofilm. One may tentatively propose some possible correspondance with Recent bacteria. The observed filamentous bacteria (type one) share morphological and size features with some sheathed bacteria (as *Sphaerotilus natans* and *Leptothrix* species) and with of some bacteria of the beggiatoales group (as *Thiothrix* species) (STROHL et al., 1989). Most of these bacteria are living in marine habitats at the interface of oxic and anoxic environments, and the sheathed bacteria are commonly encrusted with ferric iron. The coccoid bacteria (type 2) resemble some cyanobacteria as coccogonales (HUMM & WICKS, 1980) and some 'Siderocapsaceae' as *Siderocapsa* (TUOVINEN et al., 1989). All these bacteria can be coated with ferric iron precipitates but the Siderocapsaceae are more spectacular as their cells really serve as nuclei of iron deposition. Most of the cyanobacteria are living in the euphotic zone and are photoautotrophic but some are able grow in the dark heterotrophically or chemoautotrophically (being then facultatively photosynthetic) (HUMM & WICKS, 1980; BROCK et al., 1994). The Siderocapsaceae are aerobic or microaerophilic (few of them are anaerobic). Oxic-anoxic interfaces appear to preferentially colonized by these bacteria (TUOVINEN et al.,1980).

In summary, the Slivenec environments being located below the photic zone in relatively deep marine waters contain mostly grey-green limestones without any abundant bioclasts. These environments strongly suggest anoxic to dysaerobic conditions where iron would have been in its reduced state (Fe^{2+}). The presence of relatively small-sized pinkish-reddish bioclastic lenses brought during storm processes within the green limestones could have changed the local conditions. As a consequence the milieu was locally poorly oxygenated and the sediment more porous and/or more permeable allowing migration of Fe^{2+}. This iron precipitated as ferric oxides at the new anoxic/oxic interface where bacteria were living.

7 CONCLUSIONS

The iron bacteria hypothesis has the merit to be compatible with most observed pigmentation patterns. It therefore offers a reasonable explanation for the coloration of the Slivenec Limestone, as it does for the Devonian-Carboniferous Griottes or the Frasnian Marbles. These rocks are formed in different environments and contain distinct fossil assemblages. However, their pigmentation has the same origin.

ACKNOWLEDGEMENTS

The financial support of the Natural Sciences and Engineering Research Council of Canada is kindly acknowledged. The work was also financially supported by the Fonds National de la Recherche Scientifique (project FRFC n° 2-4510-96). We thank Pr. A. Bernard (Université Libre de Bruxelles, Dept. of Geology) for its support with SEM and microprobe analyses and D. Gillan (Université Libre de Bruxelles, Laboratoire de Biologie marine) for support in the interpretation of the bacterial structures.

A thorough revision of the text and constructive criticism by Joachim Reitner is gratefully acknowledged.

REFERENCES

AWRAMIC, S.M. (1982): Late Cambrian microbial endoliths of the Nopah Formation, Death Valley, California. – Geological Soc. America, Cordillera Section, Abstracts with Programs, **14**, 146, Anaheim

BEVERIDGE, T.J. & DOYLE, R.T. (1989): Metal ions and bacteria. – New York (Wiley)

BOULVAIN, F. (1989): Origine microbienne du pigment ferrugineux des monticules micritiques du Frasnien de l'Ardenne. – Ann. Soc. géol. Belgique, **112**, 79-85, Liège

-- (1993): Sédimentologie et diagenèse des monticules micritiques 'F2j' du Frasnien de l'Ardenne. - Service géol. Belgique, Prof. Paper, **1993/2-260**, 467 p., Bruxelles

BIERLEY, C.L. (1990): Metal immobilization using bacteria. – In: EHRLICH, H.L. & BIERLEY, C.L. (eds.): Microbial mineral recovery. – 303-324, New York (McGraw Hill)

BROCK, T.D., MADIGAN, M.T., MARTINKO, J.M. & PARKER J. (eds) (1994): Biology of microorganisms. – 909 p. (Prentice Hall)

BROWN, D.A., KAMENINI, D.C., SAWICKI, J.A. & BEVERIDGE, T.J. (1994): Minerals associated with biofilms occurring on exposed rock in a granitic underground research laboratory. – Appl. Environ. Microbiol. **60**, 3182-3191

CAMPBELL, S., KAZMIERCZAK, J. & GOLUBIC S. (1979): *Palaeoconchocelis starmachii* gen.n., n.sp., an endolithic rhodophyte (Bangiaceae) from the Silurian of Poland. – Acta Palaeont. Polonica, **24**, 405-408, Warsawa

CHLUPÁC, I. (1957): Faciální vyvoj a biostratigrafia Strdoceského spodního devonu.– Sbornik Ústredniho Ústavu Geologiského, **23**, 369-485, Praha

-- (1968a): Slivenec Limestones. – In: CHLUPÁC, I. (ed): Czechoslovakia, Lexique stratigraphique international. – Fascicule **6b1**, p. 326, Paris

-- (1968b): Early Paleozoic of the Bohemian Massif.– Excursion IIAC, Czechoslovakia, 43 pp., XXIII International Geol. Cong., Praha

-- (1988): Geologické zajímavosti prazskského okolí. – 249 p., Praha (Czechoslovakia Akad. Ved.)

CHLUPÁC, I., HLADIL, J. & LUKES, P. (1986): Barrandian-Moravian karst. Field Conference of the International Subcommission on Devonian Stratigraphy. A field trip Guidebook. – Ustredni Ustav geologicky, 62 p., Praha

CHLUPÁC, I., LUKES, P., PARIS, F. & SCHÖNLAUB, H.P. (1985): The Lochkovian-Pragian boundary in the Lower Devonian of the Barrandian area (Czechoslovakia). – Jb. Geol. Bundesanst., **128**, 9-41, Wien

CORSTJENS P.L., DE VRIND, J.P.M., WESTBROEK, P. & DE VRIND-DE JONG, E.W. (1992): Enzymatic iron oxidation by *Leptothrix discophora*: identification of an iron-oxidizing protein. – Appl. Environ. Microbiol. **58**, 450-454

CRICHTON, R.R. (1991): Inorganic biochemistry of iron metabolism. – 263 p. (Hellis Horwood)

DAHANAYAKE, K. & KRUMBEIN, W.E. (1986): Microbial structures in oolitic iron formations. – Mineral Deposita **21**, 85-94

DALAS E. (1990): Overgrowth of iron (III) phosphate on collagen. – J. Chem. Soc. Faraday Trans. **86**, 2967-2970

DECHO, A. W. (1994): Exopolymers in microbial mats: assessing their adaptive roles. -In: STAHL, L.J.& CAUMETTE, P. (eds): Microbial mats. – NATO ASI Series, vol. G **35**, 215-219, Berlin (Springer)

EHRLICH, H.L. (1990): Geomicrobiology of iron. -In: Geomicrobiology, 2nd ed., p. 283-346 New York (Dekker)

EMERSON, D.L. & REVSBECH, N.R. (1994): Investigation of an iron-oxidizing microbial mat community located near Aarhus, Denmark. – Applied Environmental Microbiol., **66**, 4032-4038

FRIEDMAN, E.I. (1982): Endolithic microorganisms in the Antarctic Cold Desert. – Science, **215**, 1045-1053, Washington

FRIEDMAN, E.I. & WEED, R. (1987): Microbial trace-fossil formation, biogenous and abiotic weathering in the the Antarctic Cold Desert. - Science, **236**, 703-705, Washington.

GEESEY, G.G. & JANG, L. (1989): Interactions between metal ions and capsular polymers. - In: BEVERIDGE, T.J. & DOYLE, R.J.(eds): Metal ions and bacteria. – 325-357, New York (Wiley)

GILLAN, D. & DE RIDDER, C. (1995): The microbial community associated with *Montacuta ferruginosa*, a commensal bivalve of the echinoid *Echinocardium cordatum*. – Proc. 4th Eur. Echinoderm Conf. London 1995, 71-76, Rotterdam (Balkema)

HUMM, H.J. & WICKS S.R. (1980): Introduction and guide to the marine blue green algae. -194 p., New York (Wiley)

JANNASCH, H.W. & WORSEM, C.O (1981): Morphological survey of microbial mats near deep-sea thermal vents.– Appl. Environ. Microbiol. **41**, 528-538

JUNIPER, S.K. & TEBO, B.M. (1995): Microbe-metal interactions and mineral deposition at hydrothermal vents. -In: KARL, D.M. (ed.): The microbiology of deep-sea hydrothermal vents. – 219-253, New York (C.R.C. Press)

KARL, D.M., BRITTAIN, A.M. & TILBROOK, B.D. (1989): Hydrothermal and microbial processes at Loihi Seamount, a mid-plate hotspot volcano. – Deep-Sea Res. **36**, 1655-1673

MAMET, B. & BOULVAIN, F. (1988): Remplissages bactériens de cavités biohermales frasniennes.– Bull. Soc. belge Géologie, **97**, 63-76, Bruxelles

--& --(1991): Constructions hématitiques des Griottes carbonifères (Asturies, Espagne). - Bull. Soc. belge Géologie, **99**, 229-239, Bruxelles

MAMET, B. & PERRET, M.F. (1995): Bioconstructions hématitiques de Griottes dévoniennes (Pyrénées Centrales). – Géobios, **28**/6, 655-661, Lyon

MANN, S. (1992): Bacteria and the Midas touch. – Nature, **357**, 358-359, London.

MIROUSE, R. (1992): Pyrénées Centrales franco-espagnoles. - Guides géologiques régionaux, 175pp., Paris (Masson)

MONTY, C.L., BERNET-ROLLANDE, M.C. & MAURIN, A.F. (1982): Reinterpretation of the Frasnian classical 'reefs' of the southern Ardennes – Ann. Soc. géol. Belgique, **105**, 339-341, Liège

NEU, T.R. (1994): The challenge to analyse extracellular polymers in biofilms. – In: STAHL, L.J. & CAUMETTE, P. (eds): Microbial mats. – NATO ASI Series, vol. G **35**, 221-227, Berlin (Springer)

RHEINHEIMER, G. (1980): Aquatic microbiology. – 235p., New York (Wiley)

SIMKISS, K. & Wilbur K.M. (1989): The origins of mineralization-microbial systems. – In: Biomineralization; Cell biology and mineral deposition. – 21-31 (Academic Press)

STROHL, W.R. (1989): Beggiatoales Buchanan 1957. -In: STALEY, J.T. (ed.): Bergey's manual of systematic bacteriology. – **3**, p. 2089-2110, Baltimore (Williams & Wilkins)

SVOBODA, J. & CHLUPÁC, I. (1966): Devonian. – In: SVOBODA, J. et al. (eds.): Regional Geology of Czechoslovakia. – 313-326, Praha (Czechoslovak Academy of Sciences)

SVOBODA, J. & PRANTL, F. (1950): Stratigraficko-tektonická studie okolí lomn Cikánka v Radotínském údoli. – Sbornik Stát. geolog. Ust., **27**, 105-139, Praha

TUOVINEN, O.H., HIRSCH, P. & ZAVARIN, G.A. (1989): Family ' Siderocapsaceae' Pribram 1929. – In: STALEY, J.T. (ed.): Bergey's manual of systematic bacteriology, **3**, p. 1874-1882, Baltimore (Williams & Wilkins)

WELLS M.L., PRICE, N.M. &. BRULAND, K.W (1995): Iron chemistry in seawater and its relationship to phytoplankton: a workshop report. – Mar. Chem. **48**, 157-182.

Manuscript received September 23, 1996
Revised manuscript received December 20, 1996